

Design and Implementation of a Single Grid-Current Feedback Active Damping Strategy for LCL-Filtered Grid-Connected Inverters

Fateh ABDOUNE

Centre de Recherche en Technologies Agroalimentaires, Route de Targa-Ouzemmour, Campus Universitaire, Bejaia 06000, Algeria

Corresponding author: fateh.abdoune@crtaa.dz

Abstract

This paper investigates a design method for regulating the injected current of renewable energy systems connected to the power grid through single- or three-phase voltage source inverters equipped with LCL filters. Inspired by the structure of passive damping schemes, a virtual resistance concept based on single grid-current feedback is adopted to achieve active damping without requiring additional sensors, thereby reducing system cost. Closed-loop analysis reveals that the proposed control strategy is equivalent to a conventional dual-loop control with capacitor-current feedback. However, such equivalence can only be achieved through an accurate second derivative approximation. To address the noise sensitivity associated of the derivative operation connection of a pure second derivative and a second-order low-pass filter is proposed. A proportional-resonant controller is employed to track the AC reference current, and a straightforward design procedure for determining the active damping controller parameters is introduced. To evaluate the performance of the proposed control method, the system is experimentally tested on a laboratory setup under distorted grid voltage. The obtained results confirm the effectiveness of the selected active damping approach.

Keywords

LCL filter; active damping; derivative approximation; resonant controller; stability design

1. Introduction

Distributed renewable energy sources such as photovoltaic, wind, and fuel-cell systems are commonly connected to power distribution networks through pulse-width-modulated (PWM) voltage source inverters (VSIs), which are capable of injecting controlled active and reactive power into the grid. One of the most widely used control strategies is grid-current regulation based on proportional–integral (PI) or proportional–resonant (PR) controllers [1–4]. LCL filters are commonly employed due to their cost-effective attenuation of switching harmonics. However, the resonance introduced by the LCL filter complicates the design of the current control loop and may even compromise system stability [5–7].

Numerous approaches have been proposed to mitigate this resonance issue. Among them, active damping (AD) techniques rely on an additional internal feedback loop involving one of the filter state variables, resulting in a dual-loop control structure [8–14]. Capacitor-current-feedback-based active damping has attracted significant attention because of its simplicity, effectiveness, and robustness, requiring only a proportional feedback gain [10–12]. Nevertheless, this method requires either an additional high-precision current sensor or a complex observer to estimate the capacitor current, which increases system cost and reduces overall reliability.

An alternative approach investigated in this paper relies solely on grid-side current feedback and has been shown to provide an effective and cost-efficient damping solution. Previous studies have demonstrated that damping performance comparable to proportional capacitor-current feedback can be achieved by introducing second-order derivative feedback of the grid current. However, the derivative operation significantly amplifies high-frequency noise, making practical implementation challenging. To address this issue, several studies have proposed

replacing the second-order derivative term with a first-order high-pass filter (HPF) [15–18]. Nevertheless, the co-design of the HPF and the fundamental current controller remains relatively complex and often leads to degraded dynamic performance.

Unlike previous approaches, the method proposed in this paper employs a second-order HPF to approximate the derivative term within the required frequency range, thereby simplifying the controller design while improving system performance. In addition, the closed-loop system is analyzed in the continuous-time domain, and a straightforward procedure for tuning the controller parameters is presented. Finally, the effectiveness of the proposed active damping strategy is experimentally validated on a laboratory-scale setup.

2. System Configuration and Modeling

Fig. 1 illustrates the converter system considered in this work, comprising a standard PV power system with single-phase VSI supplied by a constant DC bus voltage and connected to the grid through an LCL filter. The LCL filter is primarily designed to the guidelines in [2], and the system parameters are summarized in Table I.

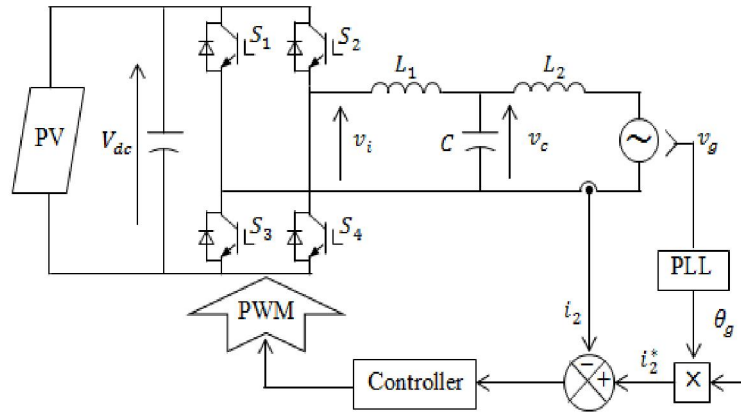


Fig. 1. Topology and control block diagram of a grid-connected VSI with an output LCL filter

For such systems, the DC-link voltage must be regulated while maintaining synchronization between the injected current and the grid voltage. This requires accurate estimation of the grid-voltage phase angle, commonly achieved using a phase-locked loop (PLL). The inverter is controlled to regulate the magnitude and phase of the grid current, thereby controlling the active and reactive power exchanged with the grid. In this study, the DC-link voltage is assumed constant and the switching frequency is considered much higher than the fundamental frequency. Under these assumptions, the state-space equations of the LCL filter can be expressed as follows:

$$\begin{aligned} sL_1 i_1(s) &= v_{in}(s) - v_c(s) \\ sC v_c(s) &= i_1(s) - i_2(s) \\ sL_2 i_2(s) &= v_c(s) - v_g(s) \end{aligned} \quad (1)$$

where L_1 is inverter-side inductance, L_2 is grid-side inductance, and C is filter capacitor. v_i denotes is inverter output voltage, i_1 the inverter current, v_c the filter capacitor voltage, i_2 the grid current and, v_g the grid voltage.

According to the superposition theorem, the transfer function relating the inverter output voltage to the injected grid current is expressed as:

$$T_{oi} = \frac{i_2(s)}{v_i(s)} = \frac{1}{sL_1 L_2 C. (s^2 + \omega_r^2)} \quad (2)$$

where ω_r is the resonance angular frequency of the LCL filter.

The system Bode diagram can be obtained from (2). It can be noted that at the resonance frequency, the LCL filter resonance causes a sharp phase drop of -180° accompanied by a high resonance peak. From a control perspective, this negative phase crossing will create a pair of closed-loop right-half plane poles, leading to

system instability. Therefore, in practical operation, an effective damping method must be employed to suppress the resonance and ensure system stability.

3. Proposed Control Approach

This section presents an active damping (AD) approach based on a virtual resistance (VR) concept derived through block-diagram manipulation. The proposed controller is selected by considering both the transient performance of the power stage and the minimization of required measuring sensors.

3.1. Developing of AD Controller

Among the possible damping-resistor locations in the LCL filter, the parallel connection across the filter capacitor provides the most suitable damping characteristics without significantly affecting the frequency response at low or high frequencies. Moreover, using single grid-current feedback eliminates the need for an additional sensor, since the grid current is already measured for power regulation. Therefore, this active damping (AD) approach offers a suitable compromise between damping performance, transient response, and implementation cost.

The corresponding block diagram for the proposed control is shown in Fig. 2, where the grid current is fed back for both injected power regulation and active damping purposes.

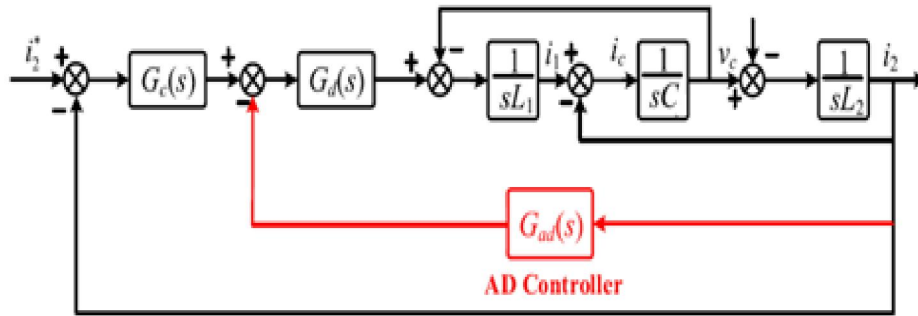


Fig. 2. Control diagram of the proposed scheme using only grid-side current feedback

In Fig. 2, $G_d(s)$ represents the control loop delay, which corresponds to 1.5 sampling periods, consisting of one sampling period of computation delay and equivalent half sampling period of zero-order-hold (ZOH) effect in PWM delays [10]. In the continuous time domain analysis, the time-delay effect is typically approximated using rational transfer functions, with the second-order Padé approximation being widely adopted. $G_c(s)$ denotes the current controller which is implemented with a PR regulator to achieve accurate tracking of the AC current reference. The AD function $G_{ad}(s)$ based on the grid-side current feedback is expressed as:

$$G_{ad}(s) = k_d L_2 C s^2 \quad (3)$$

As shown in (3), the AD function contains a second-order differential term, s^2 , which cannot be directly implemented due to possible noise amplification. Considering first that $G_{ad}(s)$ as an ideal differentiation, it can be easily identified that the proposed control structure is equivalent to a traditional dual-loop control structure with capacitor current feedback, where the damping gain k_d can be regarded as the proportion gain of the inner-loop controller. Thus, the same closed loop transfer function and so the same control effects can be achieved. It should be noted that such equivalence is obtained only with an accurate approximation of the derivative term.

3.2. Second-order Differential Approximation

The approximate term used to replace s^2 must exhibit the same frequency characteristic, especially around the resonant frequency range. It is well known that the phase angle of the s^2 term is always -180° and that its magnitude increases at a rate of 40 dB/dec. In this work, a second-order transfer function, expressed by (4), is proposed to achieve this approximation.

$$C(s) = \frac{\omega_c^2 \cdot s^2}{s^2 + \omega_c^2} \quad (4)$$

The frequency response of $C(s)$ is similar to that of s^2 over the range where the frequency is much lower than ω_c . However, it exhibits infinite gain at ω_c , which may lead to high-frequency noise amplification. To address this issue, a damping term is introduced in the denominator of (4), resulting in the following final form

$$C(s) = \frac{\omega_c^2 \cdot s^2}{s^2 + 2\zeta_0 \omega_c s + \omega_c^2} \quad (5)$$

The frequency responses of $C(s)$ and s^2 are plotted in Fig. 3, illustrating the accuracy of the proposed approximation. When a suitable ζ_0 is applied, the frequency responses of $C(s)$ coincide with s^2 in the frequency ranges around and below ω_r . A smaller ζ_0 minimizes the phase angle difference between $C(s)$ and s^2 ; however, this is accompanied by a larger gain in the high-frequency range. Conversely, a larger ζ_0 enables $C(s)$ to achieve better noise attenuation, but the damping performance is consequently weakened. Therefore, the selection of ζ_0 involves a trade-off between the accuracy of the derivative approximation and noise attenuation.

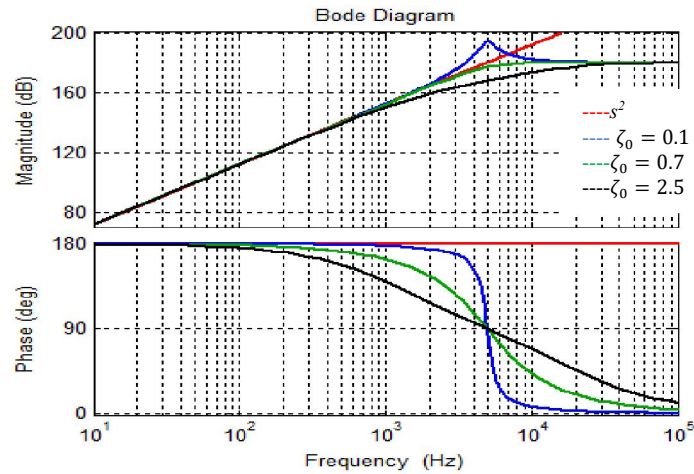


Fig. 3. Frequency responses of s^2 and $C(s)$ for different damping factor ζ_0

3.3. Closed-Loop Controller Analysis

From Fig. 2, the open-loop transfer function of the system in Laplace frequency domain can be derived as:

$$T_{1i}(s) = G_c(s) \cdot \frac{G_d(s)T_{0i}(s)}{1 + G_{ad}(s)G_d(s)T_{0i}(s)} \quad (6)$$

Frequency-domain synthesis technique can now be applied to the grid-current control loop. The frequency responses of $T_{1i}(s)$ with three different values of ζ_0 are plotted in Fig. 4. It can be observed that when $\zeta_0 = 0.7$, the resonance peak is sufficiently suppressed with a smooth phase change, indicating that system stability can be easily ensured. However, for small values of ζ_0 , even if the resonance peak is sufficiently damped, a pair of poles on the right half-plane may appear, leading to non-minimal phase behavior, which is undesirable in the control system. Therefore, a lower limit exists for ζ_0 to avoid this behavior. Conversely, when ζ_0 is large, $C(s)$ cannot approximate s^2 accurately, and the damping of the resonance is reduced, leading to an under-damped system. In this case, if the proportional gain of the current regulator is high, the system may become unstable. Hence, an upper limit for ζ_0 is also required to ensure that the resonance is sufficiently damped.

Regarding the value of ω_c , it must be set much larger than ω_r so that the AD controller exhibits the same frequency characteristics as the ideal damping controller within the range $(0, \omega_c)$. Consequently, the $G_{ad}(s)$ function can perform the damping effect around resonant frequencies. The value of ω_c should not be set excessively high to avoid undesired amplification of high-frequency noise. Following these design guidelines, ω_c is selected as $3\omega_r$ and ζ_0 is set to 0.7.

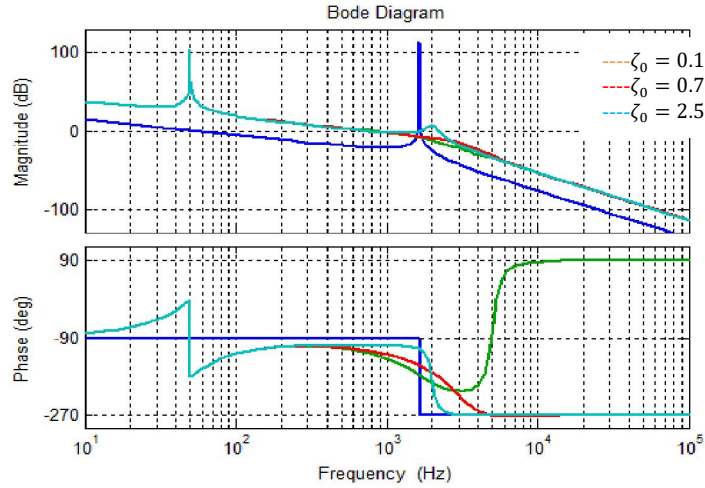


Fig. 4. Frequency response of the open-loop system considering the s^2 approximation

Based on the above analysis, two parameters need to be determined to ensure system stability in the current controller, namely k_d and k_p . The design process, which is based on the power stage characteristics and control theory, has been thoroughly explained in [3, 12]; therefore, the detailed derivation is not repeated in this paper. Based on the selected parameters, the Bode plot of the open-loop system is shown in Fig. 5. As expected, the loop gain exhibits a high magnitude characteristic in the low-frequency range, indicating that both system stability and satisfactory dynamic performance can be achieved with the proposed control method.

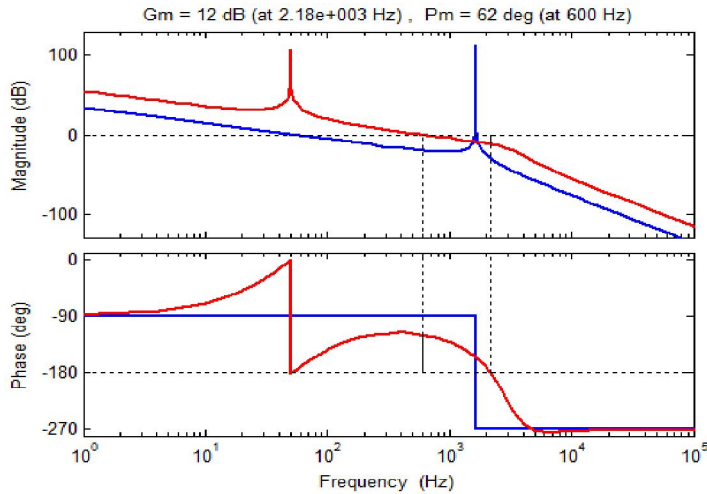


Fig. 5. Bode plot of the open-loop system with the designed PR controller

4. Experimental verification and results

The effectiveness of the proposed grid-current active damping method was experimentally verified using a laboratory prototype based on a single-phase inverter equipped with an LCL filter. The parameters of the experimental setup are listed in Table 1. The proposed closed-loop control was implemented on a dSPACE DS1202 platform, whose output gating signals are channeled to SEMIKRON inverter supplied by a constant DC power source. The grid phase voltage was detected by LV25-P sensor, while the grid-side current was measured using LA55-P sensor. An oscilloscope and power quality analyser were employed to capture and analysis the experimental waveforms.

Table.1. Parameters of the experimental setup

Parameters	Value
Grid voltage	100 V
Grid frequency	50 Hz
DC bus voltage	120 V
Nominal power	800 W
Inverter-side inductance	2 mH

Grid-side inductance	1 mH
Filter capacitance	14 μ F
Switching frequency	10 kHz

The experimental tests were conducted to evaluate the reference current tracking performance and the overall dynamic response of the proposed control. In these tests, the inverter was operated with a sinusoidal reference current at the nominal grid frequency. Fig. 6 presents the transient responses obtained when the reference current is suddenly turned on and off, respectively. It is observed that the whole system remains stable under these operating conditions. The resonance of the LCL filter is effectively suppressed, and both steady-state and transient performances are satisfactory. Furthermore, the system exhibits a very fast dynamic response, with a settling time lower than 1ms; and ensures excellent current waveform quality, as verified by the low Total Harmonic Distortion (THD) of the injected current (1.6%), even when the grid voltage contains low-order harmonics with a THD of about 5%. This high-quality performance is mainly attributed to the high loop gain at low frequencies provided by the high-bandwidth current controller, which guarantees accurate reference tracking and strong disturbance rejection capability.

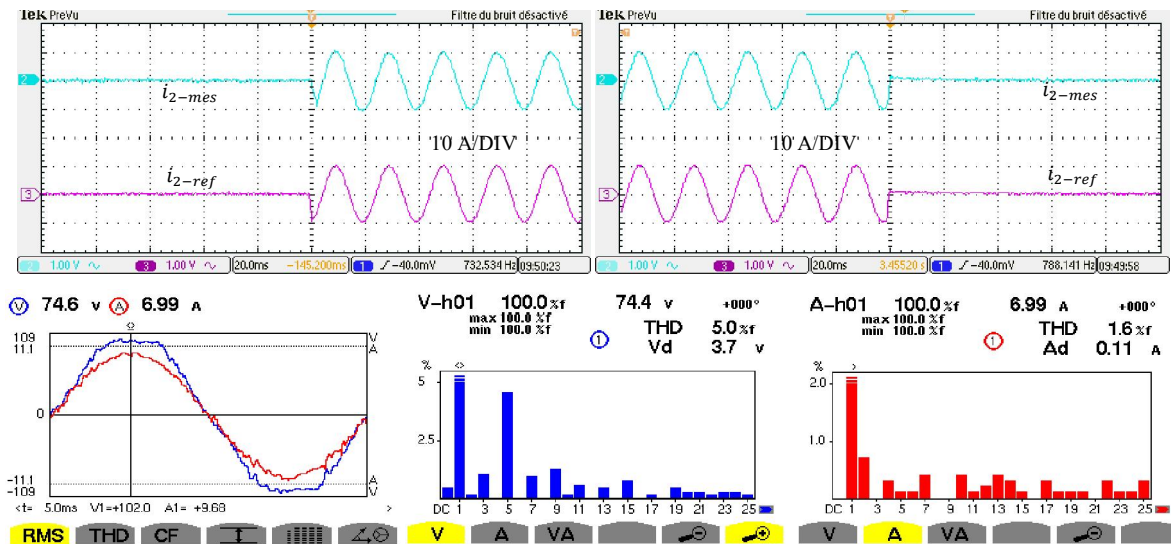


Fig. 6. Experimental transient and steady state performance of the VSI under sinusoidal reference current.

5. Conclusion

This paper has investigated a grid current feedback-based active damping strategy for LCL resonance mitigation in grid-connected VSI systems. In order to minimize the number of sensors, the grid-side current feedback is used simultaneously for regulating the injected power and actively damping the filter resonance. To address the implementation challenge caused by the second-order differential term in the controller, a second-order HPF is proposed to emulate the s^2 behavior within the desired frequency range. The controller design process, supported by theoretical stability analysis, has been presented, and the experimental validation confirms the effectiveness of the proposed control in achieving stable operation with high-quality current injection performance.

References

- [1] E. Twining and D.G Holmes, Grid current regulation of a three-phase voltage source inverter with an LCL input filter, IEEE Transactions on Power Electronics, Vol. 18, No. 3, May 2003.
- [2] B. Chenlei, L. Weiwei, P. Donghua, Control techniques for LCL type grid-connected inverters, CPSS power electronics series, Springer, 2017, ISBN: 978-981-10-4277-5.
- [3] F. Abdoune, I. Abadlia, A. Beddar, L. Hassaine, M. R. Bengourina “Analysis and Design of Voltage-controller Based on Single-state Feedback Active Damping for Grid-forming Converters”, PeriodicaPolytechnica Electrical Engineering and Computer Science, 68(1), pp. 54–63, 2024..

- [4] K. Abdoune, F. Abdoune, D. Aouzellag“Improved Voltage Harmonics Compensation Strategy for a Stand-Alone DFIG Operating under Unbalanced and Nonlinear Load Conditions”, *PeriodicaPolytechnica Electrical Engineering and Computer Science*, 64(2), pp. 144–156, 2020. <https://doi.org/10.3311/PPee.15029>
- [5] M.H. Mahlooji, H.R. Mohammadi, M. Rahimi, A review on modeling and control of grid-connected photovoltaic inverters with LCL filter, *Renewable and Sustainable Energy Reviews* 81 (2018) 563–578.
- [6] C.C. Gomes, A.F. Cupertino, H.A. Pereira, Damping techniques for grid-connected voltage source converters based on LCL filter: An overview, *Renewable and Sustainable Energy Reviews* 81 (2018) 116–135.
- [7] B. Li, W. Yao, L. Hang, L.M. Tolbert, Robust proportional resonant regulator for grid-connected voltage source inverter (VSI) using direct pole placement design method, *IET Power Electron.*, 2012, Vol. 5, Iss. .
- [8] Y. Jia, J. Zhao, X. Fu, Direct grid current control of LCL-filtered grid-connected inverter mitigating grid voltage disturbance, *IEEE Trans. On Power Electronics*, Vol. 29, No. 3, March 2014.
- [9] Y. Tang, P.C. Loh, P. Wang, Exploring inherent damping characteristic of LCL filters for three-phase grid-connected voltage source inverters, *IEEE Transactions On Power Electronics*, Vol. 27, No. 3, March 2012.
- [10] F. Liu, Y. Zhou, S. Duan, Parameter Design of a Two-Current-Loop Controller Used in a Grid-Connected Inverter System With LCL Filter, *IEEE Transactions On Industrial Electronics*, Vol. 56, No. 11, 2009.
- [11] D. Pan, X. Ruan, C. Bao, W. Li, and X. Wang, “Capacitor-current-feedback active damping with reduced computation delay for improving robustness of LCL-type grid-connected inverter,” *IEEE Trans. Power Electron.*, vol. 29, no. 7, Jul. 2014.
- [12] F. Abdoune, I. Abadlia, A. Beddar, L. Hassaine, Design and Stability Analysis of Direct Grid-Current Control for Grid-Connected Inverter with LCL Filter, *International Conference on Artificial Intelligence in Renewable Energetic Systems*, 2020.
- [13] J. Xu, S. Xie, and H. Xiao, “Research on control mechanism of active damping for LCL filters,” *Proc. Chin. Soc. Elect. Eng.*, vol. 32, no. 9, pp. 27–33, Mar. 2012.
- [14] J. He and Y. W. Li, “Generalized closed-loop control schemes with embedded virtual impedances for voltage source converters with LCL filters,” *IEEE Trans. Power Electron.*, vol. 27, no. 4, Apr. 2012.
- [15] J. Xu, S. Xie, and T. Tang, “Active damping-based control for grid connected LCL-filtered inverter with injected grid current feedback only,” *IEEE Trans. Ind. Electron.*, vol. 61, no. 9, pp. 4746–4758, Sep. 2014.
- [16] X. Wang, F. Blaabjerg, and P.C. Loh, “Grid-current-feedback active damping for LCL resonance in grid-connected voltage-source converters,” *IEEE Trans. Power Electron.*, vol. 31, no. 1, pp. 213–223, Jan. 2016.
- [17] Y. Chen et al., “Optimized design method for grid-current-feedback active damping to improve dynamic characteristic of LCL-type grid-connected inverter,” *Int. J. Electr. Power Energy Syst.*, vol. 100, 2018.
- [18] X. Zhou et al., “Robust grid-current-feedback resonance suppression method for LCL-type grid-connected inverter connected to weak grid,” *IEEE J. Emerg. Sel. Topics Power Electron.*, vol. 6, no. 4, Dec. 2018.